BNL-NUREG--35377

TI85 005126

HIGH-SPEED LWR TRANSIENTS SIMULATION FOR OPTIMIZING EMERGENCY RESPONSE*

W. Wulff, H.S. Cheng, S.V. Lekach,
A.N. Mallen, and A. Stritar
Brookhaven National Laboratory
Upton, New York 11973 (USA)

ABSTRACT

The purpose of computer-assisted emergency response in nuclear power plants, and the requirements for achieving such a response, are presented. An important requirement is the attainment of realistic high-speed plant simulations at the reactor site. Currently pursued development programs for plant simulations are reviewed. Five modeling principles are established and a criterion is presented for selecting numerical procedures and efficient computer hardware to achieve high-speed simulations. A newly developed technology for high-speed power plant simulation is described and results are presented.

It is shown that simulation speeds ten times greater than real-time process-speeds are possible, and that plant instrumentation can be made part of the computational loop in a small, on-site minicomputer.

Additional technical issues are presented which must still be resolved before the newly developed technology can be implemented in a nuclear power plant.

INTRODUCTION

The Aim of Computer-Aided Emergency Response

Operators of nuclear power plants respond to emergencies by following documented emergency procedures. Emergency procedures are carefully developed sequences of operator actions, designed to mitigate a large number of anticipated emergency scenarios. Even though the scope of emergencies covered by procedures is large and growing, the emergency potential is still larger, and an operator will always face the challenge of having to synthesize a response to unanticipated events. In such an emergency, the operator should be assisted by a computer.

The objectives of computer assistance in a power plant are (i) to monitor the plant's performance, (ii) to diagnose failures in instruments, components and systems, and (iii) to predict quickly the plant responses to several remedial operator actions after an accident. This must be achieved fast enough, so that the operator can select the optimum strategy before committing himself to a recovery maneuver. The latter two objectives are the aims of emergency assistance by computer.

Requirements for Computer-Assisted Emergency Response

Local Expertise. Emergency response is the responsibility of the operating supervisor at the plant. Only the technical staff at the power plant site has the in-depth knowledge about the plant which is essential for an emergency response. Therefore, the computing facility for emergency response must be operated with plant-specific expertise by the technical staff at the site of the plant.

On-Site Simulation Facility. It is impossible to prepare a remote central simulation facility to an emergency response at a particular plant, because invaluable time would be lost first in loading the respective instructional program and input data set, and then in synchronizing the simulations with the transient conditions in the power plant. Instead, a low-cost dedicated minicomputer must be available at the site of the power plant.

The minicomputer must be loaded with its plant-specific instructional software package and with all plant-specific data other than operating conditions. It must be continuously linked with the plant control, instrumentation and protection systems such that the dynamic simulation can be locked in step with the actual transient in the power plant, until the plant simulator or analyzer is needed for emergency response. The plant analyzer can also be made to ignore the signals from the plant and then serve for a variety of plant transient analyses and for operator training.

It would not be wise to maintain this readiness for several power plants in a single, large computer facility with a supercomputer, because all plants would be left in despair during the failure of a single computer, and remote program maintenance and upgrading for plant-specific program changes are not practical.

Fast Simulation Speeds. While plant performance monitoring can be done at real-time simulation speed, the prediction of plant responses to contemplated remedial actions in emergency situations requires much faster simulation speeds. Simulation speeds of ten times faster than real-time speeds or higher must be achieved without loss in frequency response. High computing speeds are routinely obtained for slow, quasi-static events. They are also needed for rapid transients in severe accidents.

On-Line Link with Reactor. As discussed above, the plant analyzer must be linked with plant control and protection systems via one-way optical data transfer channels and with the control room instrumentation so that the transient in the power plant can be reproduced in the analyzer until a prediction is needed in an emergency.

This requirement should not be confused with the task of establishing the steady-state conditions in the plant from a few operating conditions because a transient starting condition is defined only by the

*Work performed under the auspices of the U.S. Nuclear Regulatory Commission.

complete set of all state variables for the system. It is therefore necessary to isolate from the entire plant that portion which must be dynamically simulated for an emergency in the nuclear steam supply system. Then one must define the boundary interfaces between the simulated portion and the remainder of the system. These interfaces are invariable control actuator positions for valves, relays, etc., and must be communicated on demand to the plant analyzer.

The communication channels must be scanned during every computational cycle, to assure computational continuity and fidelity. The computational cycling frequency must be approximately an order of magnitude greater than the expected simulation response frequency.

The plant analyzer must offer a large number of computed parameters from which the operator can select any one for convenient graphical display.

Scope of Paper

From all the above requirements imposed on a nuclear power plant analyzer or simulator for emergency response, the requirements of high-speed realistic simulations of severe transients in a low-cost minicomputer are the most difficult ones to achieve. We present first a summary of previously used and currently contemplated approaches to nuclear power plant simulation, then we report on a newly developed technology and present an assessment of its capabilities.

CURRENT APPROACHES TO HIGH SIMULATION SPEED

Real-time simulation speed has been sought by manufacturers of training simulators, by vendors for the design of nuclear power plants and, on behalf of the Nuclear Regulatory Commission, by the developers of codes for safety analyses in national laboratories. Real-time simulation speed can be achieved only by matching modeling and programming techniques with computer capabilities.

Modeling

The mathematical models for training simulators were simplified in the past to achieve real-time simulation speed with available computing power. Rates of change (for fission power, for example [1]) have been artificially limited and coolant inertia has been ignored [1] to maintain computational stability. Such modeling restrictions are now being eliminated as faster minicomputers become available.

The need for increased computing speed has had almost no impact on the modeling in the major systems codes TRAC [2] and RELAP-5 [3], developed by Los Alamos National Laboratory and Idaho National Engineering Laboratory, respectively, for the U.S. Nuclear Regulatory Commission. The models are based on standard finite differencing of partial differential equations for the two-phase coolant mixture. Increases in computing speed have been sought by remodeling the power plant with fewer computational cells. Finite difference methods, however, converge to the correct solution only as the mesh size and the time step decrease toward zero. As expected, any significant reduction of the cell number leads to significant losses in accuracy [4]. Analytical methods have rarely been used in the past to increase simulation efficiently [5].

Numerical Integration

Major efforts have been made to improve the integration algorithms for greater execution speed, particularly in codes which use matrix inversions for solving large systems of nonlinear equations, such as TRAC and RELAP-5. A linearization technique has been used to replace the matrix of rank (MN), representing M field equations in N computational cells, before its inversion by a matrix of rank N for the pressure field. This reduces drastically the computational effort for integrating all field equations. The method fails, however, when partial derivatives of coolant properties vanish or tend toward infinity. With this method one cannot realize the computational savings arising from the behavior of incompressible fluids.

Predictor-corrector methods, traditionally used for integrating ordinary differential equations, have also been used for integrating partial differential equations faster in the fast version TRAC-PF1 [2].

PROGRAMMING LANGUAGE

One must always choose between computing efficiency and program transportability. Computer codes written in standard FORTRAN can readily be made to execute on any large computer, yet they can never utilize fully the architecture of a particular computer. FORTRAN compilers have been developed for several computers with parallel and/or pipeline execution, but they do not produce efficient machine codes unless the programmer adheres to very detailed and machine-dependent constraints which render the code machine-specific. The Cray-1 supercomputer executes for a dense linear system [6] from two to six million floating point operations when programmed in standard FORTRAN. Specialized Vector FORTRAN for the Cray machine executes up to six times faster, Vector Assembly Language up to twenty times faster, but only on the Cray machine. One can have either an efficient code, or a transportable code.

Program transportability has always been given a higher priority than execution efficiency by vendors of training simulators, by power plant designers and in government-sponsored code developments for reactor safety analyses. There is widespread apprehension against unfamiliar, non-FORTRAN programming languages in the nuclear industry which is unparalleled in non-nuclear simulation activities.

Computers

There are two trends in the selection of computers for nuclear power plant simulations. Vendors of training simulators seek to employ minicomputers with increasing computing power, accomplished by parallel processing in pipelined computer architectures. In contrast, for almost all major systems codes, developed on behalf of the Nuclear Regulatory Commission, the trend is from large mainframe computers such as the CDC-7600 to even larger super computers such as the Cray computer. Simulations are largely carried out on general-purpose computers with standard FORTRAN programs. However, this paper deals with a power plant simulation on a modern special-purpose peripheral processor which was specifically designed for systems simulation.

Graphic Display Systems. The advantage of multicolor graphics for input and output processing has been widely accepted because it has the potential of reducing sharply the first and last of the three time-consuming operations in simulation, which are input data preparations, program execution and evaluation of output data.

NEWLY DEVELOPED HIGH-SPEED SIMULATION TECHNOLOGY

The careful selection of modeling and programming techniques and the deliberate choice of a particularly suitable, special-purpose minicomputer produced a new plant analyzer for realistic simulations of normal and severe abnormal transients in nuclear power plants. The most prominent distinctions of the plant analyzer are its great simulation speed, its low capital and operating costs, its outstanding user conveniences and its unsurpassed ability to accommodate control and instrumentation signals in analog or digital form.

The plant analyzer was developed for BWR power plant simulations. The simulation principles employed, however, are general and apply to all power plant simulations.

Modeling Techniques

The most demanding part of light water reactor plant simulation is the modeling of the two-phase flow thermohydraulics in the reactor vessel and, if appropriate, in the steam generators. The coolant dynamics, therefore, dominate the selection of modeling strategy, mathematical methods and computer hardware.

The balance of plant simulation, while taxing computing capacity and input/output processing, is effectively achieved with familiar mathematical models. The simulation of neutron kinetics may require special attention. The plant analyzer described herein employs point kinetics, requiring a relatively small simulation effort. Multidimensional kinetics simulation, however, can also be achieved with standard models and a suitable peripheral processor. Here, the focus of power plant simulation is on the coolant thermohydraulics.

Modeling Principles. Modeling efficiency is achieved when the greatest possible simulation fidelity is produced with the smallest possible number of arithmetic operations. It is achieved by:

(i) selecting the least complicated thermohydraulics model for two-phase flow which accommodates all the available experimental information on two-phase flow,

(ii) eliminating from the models all irrelevant phenomena, while accounting for all possible flow patterns and important processess,

(iii) executing as many integrations as possible in analytical form and evaluating the analytical solutions dynamically during the simulation,

(iv) executing in advance all iterative procedures required for the solution of implicit sets of nonlinear equations, then tabulating the results in terms of explicitly known variables and interpolating the tables during the simulation.

(v) combining analytically in every equation all constitutive relations (material properties, correlations, etc.) into the smallest possible number of expressions and tabulating the expressions for interpolation during the simulation.

The first of these five principles suggests to use only field equations with known mass, momentum and energy interphase and wall to fluid transfer terms that can be modeled and validated with currently available instrumentation [7], since otherwise such field equations only burden the computations, without producing reliable information. By adhering to the fourth and fifth principles one takes advantage of low-cost central core memory now available even in modern minicomputers, and one reduces many computations of any complexity to evaluations of linear expressions. All five principles require some engineering judgement and developmental efforts but, together with proper selections of computing methods and processors, they contribute significantly to efficient high-speed simulation. Below we demonstrate how these principles have been applied in the plant analyzer. For a complete description of the models see Reference [8].

Coolant Hydraulics. For the BWR plant analyzer development described herein, it was recognized [8] that phase separation, coolant mixture level tracking, nonequilibrium boiling, flashing and condensing, and particularly the tight coupling between fission power and vapor void fraction in the reactor core are the most important aspects of coolant dynamics modeling. Acoustical effects in the steam lines are deemed to be important, while acoustical effects in the liquid phase of the coolant mixture are unimportant.

Following the first modeling principle, we selected the four-equation drift flux model which consists of the vapor mass balance and the three balance equations for mixture mass, momentum and energy. Following the second principle and recognizing the irrelevance of acoustical effects in the liquid, we decided to use the volume-averaged vessel pressure*

$$\langle p\rangle = \frac{1}{V_v}\int_{V_v} p\,dV \qquad (1)$$

to compute all thermophysical coolant properties. The vessel pressure is computed by combining the mixture mass balance, expressed as the volumetric flux divergence equation,

$$\nabla \vec{j}_m = \frac{\rho_\ell - \rho_g}{\rho_\ell \rho_g}\Gamma_v - \left[\frac{\alpha}{\rho_g}\frac{D_g\rho_g}{D\tau} + \frac{(1-\alpha)}{\rho_\ell}\frac{D_\ell\rho_\ell}{D\tau}\right], \qquad (2)$$

with the caloric equations of state for liquid and vapor, and with the phasic energy balance for the liquid, and by integrating the resulting ordinary differential equation

$$\dot{\langle p\rangle} = \{(Aj)_{fw} - (Aj)_{s\ell} + \sum(Aj)_{inj} + \int_{V_2}\frac{\rho_\ell - \rho_g}{\rho_\ell\rho_g}\Gamma_v dV -$$

$$\frac{1}{\rho_\ell^2}\left(\frac{\partial\rho}{\partial u}\right)_p\left[\int_{A_1} q_w'' dA + \int_{V_1} q_\ell''' dV\right]\}/$$

$$\left[\int_{V_2}\alpha\frac{\rho_g'}{\rho_g}dV + \int_{V_1}\frac{1}{\rho_\ell}\left(\frac{\partial\rho_\ell}{\partial p}\right)_u dV\right]. \qquad (3)$$

Following the third principle, we integrated Equation 2 analytically to replace the partial differential equation of mixture mass conservation by this quadrature in space

*All symbols are defined in the Nomenclature at the end of the paper.

$$j_m(z) = j_m(o) + \frac{\rho_\ell - \rho_g}{\rho_\ell \rho_g} \int_o^z \Gamma_v d\tilde{z} - \frac{\rho_g^{\prime}}{\rho_g} \langle \dot{p} \rangle \int_o^z \alpha d\tilde{z}$$

$$- \frac{1}{\rho_\ell^2} \left(\frac{\partial \rho_\ell}{\partial u}\right)_p \left\{ \int_o^z (1-\alpha) q_w'' \frac{C}{A} d\tilde{z} - h_{fg} \int_o^z \Gamma_v d\tilde{z} \right.$$

$$\left. + \int_o^z (\alpha - 1) q_\ell''' dz \right\} . \qquad (4)$$

The time-dependent starting value $j_m(o)$ is computed from the momentum equation. Satisfying again the third principle, we integrated analytically the momentum balance

$$\frac{\partial G_m}{\partial \tau} + \frac{\partial}{\partial z} \left[\alpha \rho_g w_g^2 + (1-\alpha)\rho_\ell w_\ell^2\right] + \frac{\partial p}{\partial z} + g_z \rho_m$$

$$+ f_{\ell o} \phi_{\ell o}^2 \frac{G_m |G_m|}{2 d_h \rho_\ell} = 0 \qquad (5)$$

along every straight stream-tube segment of every closed flow contour in the vessel and recirculation loops, linked the results to eliminate the pressures at segment terminals and thereby replaced Equation 5 in every computational cell by three loop momentum balances

$$\frac{d\mathcal{M}_j}{d\tau} = \Delta p_{JTP} - \sum_{i=1}^{N_{s,j}} \left\{ g_z \langle \rho_m \rangle + \frac{1}{2 d_h} \int_o^L \frac{f_{\ell o} \phi_{\ell o}^2}{\rho_\ell} G_m |G_m| dz \right\}_{ij} +$$

$$\frac{1}{2} \sum_{\substack{i=1 \\ i \neq JTP}}^{N_{s,i}} \left\{ (w_\ell G_\ell + w_g G_g)^+ - (w_\ell G_\ell + w_g G_g)^- \cdot \right.$$

$$\left. \left[1 + \left(\frac{A^-}{A_{min}}\right)^2 \zeta\right] \right\}_{ij} , \quad j = 1,\ldots,3 \qquad (6)$$

for the vessel and a similar one for the recirculation loop. The loop momentum in Equation 6 is defined by

$$\mathcal{M}_j = \sum_{i=1}^{N_{s,i}} \int_o^{L_{ij}} G_m(z)\, dz , \qquad (7)$$

and the mixture, vapor and liquid mass fluxes are related to the mixture volume flux in Equation 4 by, respectively,

$$\left.\begin{aligned} G_g &= w_g \rho_g = \rho_g \left(f_1 \langle j_m \rangle + f_2\right) \\ G_\ell &= w_\ell \rho_\ell = \rho_\ell \left[(1-f_1) \langle j_m \rangle - f_2\right] \\ G_m &= \left[\rho_\ell - f_1 (\rho_\ell - \rho_g)\right] \langle j_m \rangle - f_2 (\rho_\ell - \rho_g), \end{aligned}\right\} \qquad (8)$$

where $f_1 = C_o \langle \alpha \rangle , \; f_2 = \langle \alpha \rangle \langle\langle V_{gj} \rangle\rangle$. (9)

Notice that Equation 6 accounts fully for gravity effects, wall shear, momentum flux and form losses. It predicts natural circulation but not the unimportant propagation of acoustical waves. Equation 6 not only replaces the expensive task of integrating, for example, as many as fifty-four momentum equations for fifty-four vessel cells by the simpler task of integrating three momentum equations for three loops, covering all fifty-four cells, but it also reduces drastically the computational stiffness of the mathematical model. Only in the steam line does the plant analyzer integrate the momentum balance in finite-difference form for each one of ten computational cells [8].

The use of Equations 3, 4 and 6 reduces the need for integrating the 216 differential equations of the four-equation model for fifty-four computational cells, to the much simpler task of integrating only 111 differential equations. These are the three loop momentum balances (Equations 6), and fifty-four each of the vapor mass balances

$$\left(\frac{dm_g}{d\tau}\right)_j = V_j \langle \Gamma_v \rangle_j + (AG_g)_{j-1} - (AG_g)_j , \qquad (10)$$

$$j = 1,\ldots,54$$

and of the mixture energy balances

$$V_j \left(\frac{d\langle u_m \rho_m \rangle}{d\tau}\right)_j = \left[A(G_\ell h_\ell + G_g h_g)\right]_{j-1} - \left[A(G_\ell h_\ell + G_g h_g)\right]_j$$

$$+ L_j \left[\langle q_w'' \rangle + A \langle (1-\alpha) q_\ell''' \rangle\right]_j ,$$

$$i = 1,\ldots,54 . \qquad (11)$$

Further details, specifically on constitutive relations for vapor generation and heat transfer, are found in Reference [8].

<u>Conduction in Fuel Elements</u>. Following once again the third modeling principle, we integrated the transient conduction equation for radial conduction of heat, over the cross sections of fuel pellet, gas gap and fuel cladding to obtain an ordinary differential equation [8,9] for the rate of fuel temperature change:

$$\frac{d\langle T \rangle}{d\tau} = \frac{2}{sR_w} \frac{\tilde{k}_{c\ell}}{(\widetilde{\rho c})_{f\ell}} \frac{N_{Bi}(T_\infty - \langle T \rangle)}{1 + N_{Bi}(C_g + F_{pr})} + \left(\frac{R_1}{R_w}\right)^2 \frac{\langle q''' \rangle_f}{(\widetilde{\rho c})_{f\ell}} \qquad (12)$$

where $N_{Bi} = h_c s / k_{c\ell}$ is the cladding Biot number, C_g is a constant depending on geometry and F_{pr} is a function of thermal properties [8]. Equation 12 is integrated for every axial fuel element (twelve in each channel) and then used to compute for each axial element the radial temperature distributions. In the fuel pellet the distribution is, with $\zeta = r/R_1$

$$T_{f\ell} - T_\infty = \left\{1 + N_{Bi} \left[\frac{R_w}{R_m} + \frac{R_w}{R_i} \frac{\tilde{k}_{c\ell}}{s} \left(\frac{\delta}{k}\right)_g + \frac{\tilde{k}_{c\ell}}{2\tilde{k}_f} \frac{R_w}{s} (1-\zeta^2)\right]\right\}$$

$$\cdot (T_w - T_\infty) , \qquad (13)$$

and in the cladding the distribution is, with $\eta = (r - R_1)/s$

$$T_{c\ell} - T_\infty = \left[1 + N_{Bi} \frac{R_w}{R_m} (1-\eta)\right] (T_w - T_\infty) . \qquad (14)$$

In Equations 13 and 14

$$T_w - T_\infty = (\langle T \rangle - T_\infty) / \left[1 + N_{Bi} (C_g + F_{pr})\right] \qquad (15)$$

is the excess wall temperature above the coolant temperature T_∞.

Equation 15 is implicit in T_w because the heat transfer coefficient $\bar{h}_c$ in the Biot number and the material properties in F_{pr} depend on T_w. Therefore, the calculation of the right-hand side of Equation 12 and of Equations 13 through 15 requires an iterative procedure, involving the selection of the appropriate heat transfer regime and the evaluation of the corresponding heat transfer correlation. Following the fourth modeling principle, the excess wall temperature is computed in advance by Newton-Raphson iteration, over the entire range of possible fuel temperatures and flow conditions. The result is stored in a multi-dimensional table, with known variables as table entries. The evaluation of transcendental expressions is thereby reduced to a time-saving linear interpolation of a nonlinear table. A single table accounts, without loss in accuracy, for all the material properties and heat transfer correlations [8], regardless of their complexity.

Turbine Models. In order to predict the turbine power and the steam exit enthalpy from inlet conditions, turbine speed and exit pressure, one must compute the isentropic enthalpy drop and the thermodynamic turbine efficiency [8]. Following the third modeling principle, we integrate Gibbs' equation

$$T ds_m = dh_m - dp/\rho_m \tag{16}$$

along an isentrope, from the inlet condition $\{(h_m)_i, p_i\}$ to the exit pressure p_e and find

$$\Delta h_{is} = (h_m)_i \left[\frac{T_s(p_e)}{T_s(p_i)} - 1 \right] + T_s(p_e) \left\{ \int_{p_i}^{p_e} \frac{v_f}{T_s} dp - \int_{T_s(p_i)}^{T_s(p_e)} h_f \frac{dT_s}{T_s^2} \right\} . \tag{17}$$

Equation 17 is evaluated by closed-form integration, with known polynomials for the saturation properties. Following the fifth modeling principle, we tabulated the term in square brackets and the last term in Equation 17, each as a two-place function. Thus, the isentropic enthalpy drop in the turbine is computed rigorously by evaluating linear expressions in $(h_m)_i$, p_i and p_e.

Adhering again to the fifth principle, the turbine speed-dependent thermodynamic efficiency is evaluated for a set of nine fixed coefficients of a particular stage, specifying the theoretical degree of reaction, the rotor entrance flow angle, the mean radius ratio, the meridian velocity ratio, the losses in rotor and stator, the reheat factor and the kinetic energy recoveries [8], and as a function of the ratio $\nu = U_1/\sqrt{2\Delta h_{is}}$ of rotor speed over maximum steam velocity. Here, a single linear interpolation produces the result of two square root extractions, the evaluation of a trigonometric function and over fifty additions, subtractions and multiplications.

Feedwater Preheaters. The feedwater temperature rise in the combination of a main heat exchanger and a drain cooler is computed from analytical integrations of the energy balances for the fluids on the shell and tube sides. The result is dynamically evaluated during the simulation, as called for by the third modeling principle:

$$(T_{fw})_e - (T_{fw})_e = \left[(T_s)_c - (T_{fw})_i\right] \cdot f_{FWH} , \tag{18}$$

where

$$f_{FWH} = \frac{e^m (\mu - 1)}{\mu e^m - 1} (1 - e^n) , \tag{19}$$

$$m = (AU)_D \left[1/W_{SHS} - 1/W_{fw}\right]/c_p ; \; n = (AU)_H/(c_p W_{fw}) . \tag{20}$$

Effects of thermal storage and transport times are modeled as a first-order time lag. Individual heater failures are also modeled.

Other Components. The five modeling principles listed above have been employed for the nuclear steam supply system, the balance of plant components, the control systems and the plant protection systems. While ordinary differential equations are used to predict angular speeds in pumps, turbines, electric motors and generators, control functions and valve positions, all nonlinear characteristics for induction motors, pumps and valves are precomputed from first principles or generally applicable empirical correlations and tabulated for linear interpolation in the plant analyzer [8].

Selection of Computing Methods and Computer

The computing method and the special-purpose processor have been chosen for the plant analyzer to achieve the greatest possible simulation speed in a minicomputer. The choice of suitable algorithms for the numerical simulation and of the corresponding processor are, however, intimately related to the form of the mathematical models. As explained above, physics dictated the selection of the four-equation mixture model for coolant dynamics. This four-equation model was then cast in the form of ordinary differential equations (cf Eqs. 3, 6, 12 and particularly Eqs. 10 and 11). This form, and also the fourth and fifth modeling principles established earlier, suggest strongly simulation procedures and computer characteristics, the selection of which is discussed below.

First, we decided whether to integrate explicitly or implicitly, and then we selected a suitable digital computer. A numerical integration procedure is called explicit if the values of all state variables for a future time level are computed explicitly in terms of state variable values only from the past and present time levels. Such a procedure requires no iteration on state variables.* All other numerical integration procedures are called implicit, lead to nonlinear difference equations and require iterations for every time step.

The rational choice between explicit or implicit integration is based upon estimates of these three measures:

(i) the most predominantly encountered high-frequency (f_ν) content of input data and computed parameters,

(ii) the permissible integration step size $\Delta\tau_{int}$ and

(iii) the frame time $\Delta\tau_{frm}$ needed by the computer to advance the simulation from one time level to the next.

*Minor iterations may be necessary to calculate subsidiary variables (cf. Eq. 15).

Frequency Content. Of all the processes driving the system transients, the one with the highest natural frequency f_ν must be accurately simulated and therefore imposes an upper limit $\Delta\tau_\nu = 1/(5f_\nu)^*$ on the integration step size $\Delta\tau_{int}$. This limit must be imposed over and above applicable limits arising from numerical stability or form truncation errors.

Neutron kinetics has the highest frequency, but it is not a driving mechanism in a BWR power plant. Instead, prompt fission follows the relevant driving mechanism of acoustics in the steam line. In a BWR-4 plant the pressure oscillations reach the frequency of approximately $f_\nu = 10$ Hz.

Permissible Integration Step Size. The highest possible simulation speed is achieved with the largest permissible integration step size

$$\Delta\tau_{int} = \mathrm{Min}\ \{\Delta\tau_a, \Delta\tau_s, \Delta\tau_\nu\}\ , \tag{21}$$

where $\Delta\tau_a$ is the limit required to maintain accuracy by controlling the truncation errors inherent in all finite difference analogues for derivatives, $\Delta\tau_s$ is the stability limit imposed to avoid exponential growth of round-off errors, and $\Delta\tau_\nu$ is the limit imposed to simulate accurately the high frequency content of driving processes or of boundary conditions. The first two limits characterize the integrating algorithm and depend on its time-dependent eigenvalues. The third limit characterizes the system to be simulated. The first and last limits are related to each other via the same high-order time derivatives of the mathematical model.

For unconditionally stable integrating algorithms $\Delta\tau_s$ is obviously unbounded. Most implicit algorithms have this desirable feature, while explicit integrations are conditionally stable with a bounded $\Delta\tau_s$.

Frame Time. $\Delta\tau_{frm}$ is the clock time that the computer needs to execute all computations for the advancement of the simulation from one time level at τ to the next level at $\tau + \Delta\tau_{int}$. The frame time for implicit integration is always much larger than for explicit integration because of time-consuming iterations.

If the model is formulated, the number of arithmetic operations is established and the frame time can be predicted from given processing speeds. Most computer vendors specify maximum execution speeds (in million floating point operations per seconds, for example) but such specifications are useless because of the uncertainty in the utilization of maximum processing rates. Only Applied Dynamics International of Ann Arbor, Michigan, specifies the time requirement for each operation in sufficient detail for reliable frame time estimates.

Computing Speed. Once the above three measures have been estimated one can easily compute the simulation speed as the multiple S of real-time process speed:

$$S = \Delta\tau_{int}/\Delta\tau_{frm}\ . \tag{22}$$

*The factor 5 applies here to a third-order Adams-Bashford integration routine and may be greater for lower-order algorithms.

It is clear that if $\Delta\tau_\nu$ is small, explicit integration with its small $\Delta\tau_{frm}$ produces the larger ratio S, while unconditionally stable, implicit algorithms simulate quasi-steady transients faster.

Computing Method for Plant Analyzer. Computing experience with TRAC and RELAP-5 codes lead to an estimate of the frame time $\Delta\tau_{frm}$. An implicit integration of four field equations for approximately one hundred computational cells would require a frame time of 180 milliseconds on a large mainframe, general-purpose computer (CDC-7600) or 160 to 700 milliseconds on an array processor programmed in FORTRAN. An explicit integration of the same problem requires approximately 30 milliseconds on a general-purpose computer and 6 milliseconds on available array processors designed specifically for explicit integrations.

Since $\Delta\tau_{int}$ in Equation 22 is limited, according to Equation 21, to $\Delta\tau_\nu = 50$ milliseconds for both explicit and implicit integrations, it is clear that explicit integration produces the higher speed-up factor S in Equation 22. Therefore, explicit integration was chosen for the plant analyzer.

Implicit integration is of interest only when $\Delta\tau_\nu$ and $\Delta\tau_a$ in Equation 21 are much larger than 180 milliseconds. To achieve ten times real-time simulation speed ($S = 10$) with implicit integration, one would have to limit the range of simulated transients to those whose frequency content is below 0.1 Hz, and one would have to use a large mainframe computer.

Computer Selection for Plant Analyzer. Implicit integration involves matrix inversions which are best accomplished in array processors with two or more central processsing units, because the elementary row operations of matrix inversion involve parallel column operations, similar to signal processing. Explicit integration, on the other hand, is best accomplished in a special-purpose peripheral processor which has the inherent characteristics of an analog computer and the integrating capacity and stability of a digital minicomputer.

With the explicit integration method selected, a nationwide search was launched for the most suitable minicomputer to execute high-speed integration of large systems of nonlinear explicit first-order ordinary differential equations. The AD10 of Applied Dynamics International in Ann Arbor, Michigan emerged as the most suitable minicomputer available in 1981. Two AD10 units have been installed at BNL and are operational since March 1982.

Major Characteristics of Plant Analyzer

A detailed description of the AD10 architecture is beyond the scope of this paper but can be found elsewhere [8,10]. In brief, the AD10 is a special-purpose peripheral array processor, designed for high-speed simulation of large complex systems by integration of nonlinear ordinary differential equations. The AD10 is programmed via a host computer, a PDP or VAX minicomputer.

The AD10 contains six distinct, task-specific processors which operate in parallel and are synchronized at the computing cycle frequency of 10 MHz. The six processors serve (i) to link the AD10 with the host computer, (ii) to time and control the other five processors, (iii) to execute logical decisions and binary searches for table interpolation (iv) to execute additions, subtractions and multiplications in integer or fractional arithmetic, (v) to carry out numerical integrations, and (vi) to address memory. Two additions and one multiplication can be carried out in one cycle, resulting in thirty million fractional operations per second. Twenty million words can be transferred each second between memory and processors. Internally generated digital data can be issued as digital data at the rate of 3 million words per second or converted to analog signals in the range from -10 volt to +10 volt. Input signals can be accepted as digital (3 million words per second) or analog signals (± 10 volt).

Capabilities. The two AD10 processors installed at BNL can integrate as many as 1,950 state equations, with any combination of seventeen built-in algorithms, such as first through fourth orders Adams-Bashford or Adams-Moulton and second through fourth orders Runge-Kutta procedures. The mix of algorithms can be altered with a single keyboard command, on-line and without reloading the program.

The two processors can generate as many as 18 nonlinear functions of one variable, plus 34 functions of two variables, plus 12 functions of three variables in as little as 98 microseconds, regardless of the functions complexity. This feature is utilized by Modeling Principles iv and v.

Up to 256 input and output analog channels can be scanned for every computing frame. This makes the outside world (instrumentation and controls in a power plant) part of central core memory.

The BWR plant simulation presented here entails 320 integrations with 4,000 subroutine or module calls, including the interpolation of over 200 nonlinear multidimensional tables, many as often as 54 times during every computing frame. All of this is achieved in the frame time $\Delta\tau_{frm} = 5.4$ ms. The maximum integration step size is $\Delta\tau_{int} = 54$ ms, producing a ten times greater than real-time simulation speed (cf. Eq. 22). Twenty-eight analog channels are scanned 200 times per second to introduce operator actions and malfunctions any time before or during the simulation. Sixteen output channels are currently updated 200 times per second for graphic display and storage of computed results. This capability is indispensible for computer-aided emergency response.

Limitations. The AD10 processors installed at BNL* employ 16-bit integer arithmetic in all but the integrating processors (which have a 48-bit mantissa in pseudo floating point representation). The 16-bit integer arithmetic not only requires scaling of all variables, but also limits the dynamic range to two decades if the relative error is kept below 1/2%. All variables are scaled to fall in the range [-1, +1]. The least significant bit is $2^{-15} = 3 \times 10^{-5}$.

Scaling means additional analytical work during program implementation. One is rewarded, however, from this scaling work by gaining in-depth understanding of the mathematical models and by obtaining a solid basis for program validation.

*A new floating-point processor FX is now available with greater computing speed and capacity, at the same cost.

We have employed dynamic scaling for one parameter only, to expand its dynamic range from two to five decades. Assume that in the scaled equation

$$\overline{y} = C\ \overline{f}(\overline{x}) \ , \ -1 \leq \overline{x} \leq +1 \qquad 0 \leq |C| \leq 512, \text{ constant} \tag{23}$$

$|\overline{f}|$ reaches the noise level for $\overline{x} \in [a,b]$. Then

$$\overline{y} = C\cdot\overline{f}(\overline{x})\cdot\overline{p}(\overline{x}) + \frac{C}{1000}\left[1000\cdot\overline{f}(\overline{x})\right]\left[1-\overline{p}(x)\right],$$

$$\text{where} \quad \overline{p}(\overline{x}) = 1 \text{ for } \overline{x} \in [-1,a) \text{ and } \overline{x} \in (b,1] \qquad \overline{p}(\overline{x}) = 0 \text{ for } \overline{x} \in [a,b] \ , \tag{24}$$

has a dynamic range which is three decades larger than that of Equation 23.

Programming Language. The AD10 is not a general-purpose computer, programmable in general-purpose FORTRAN. The AD10's own high-level systems simulation language MPS-10 consists of subroutine or module calls which reflect analog computer operations. The major advantage of MPS-10 is that it contains a single rule with which to utilize fully the parallel and pipelined processing in the AD10 Module calls need only to be packaged in groups, called Data Areas, until such groups are filled up. Then all overhead operations are minimized, pipe lines are fully utilized and the maximum simulation speed is achieved, unless one cares to program in assembly language. MPS-10 is relatively easy to learn.

Graphic Display. Currently we transmit any set of fifteen parameters and time to an expanded IBM Personal Computer (PC) for storage and subsequent display in labelled diagrams on a four color CRT monitor. Any two of the fifteen parameters can be selected for online display during the simulation. A dot matrix printer produces black and white hard copies of the monitor image.

Any variable can be displayed also on a Type 4012 Tektronix storage oscilloscope with thermal printer. The oscilloscope is the primary display device for program development and interactive system analysis.

ACHIEVEMENTS OF HIGH-SPEED SIMULATION

Scope

Figure 1 shows schematically the BWR-4 plant configuration simulated for this paper. Shown are the reactor, the balance-of-plant components and the control system, i.e., the pressure regulator (P), the feedwater regulator (FW) and the recirculation flow controller (FW). The arrangement of computational cells in the vessel is shown in Figure 2.

The simulation encompasses neutron kinetics, thermal conduction in fuel structures, nonhomogeneous, nonequilibrium coolant dynamics with level tracking, boron transport, the dynamics of steam line flow, turbines, condensers, feedwater preheaters, turbine-driven feedwater pumps, pump speed-controlled recirculation flows, suppression pool, plant protection systems and the control system described above [8].

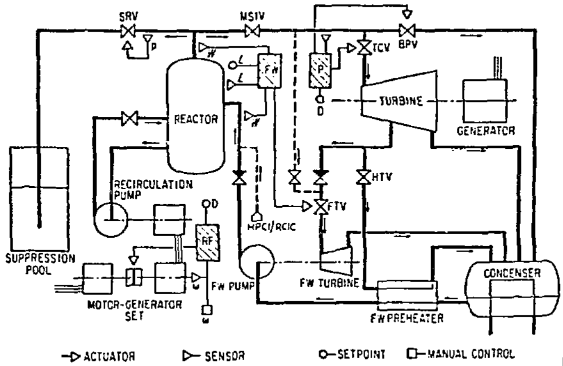

Figure 1 BWR Plant Schematic

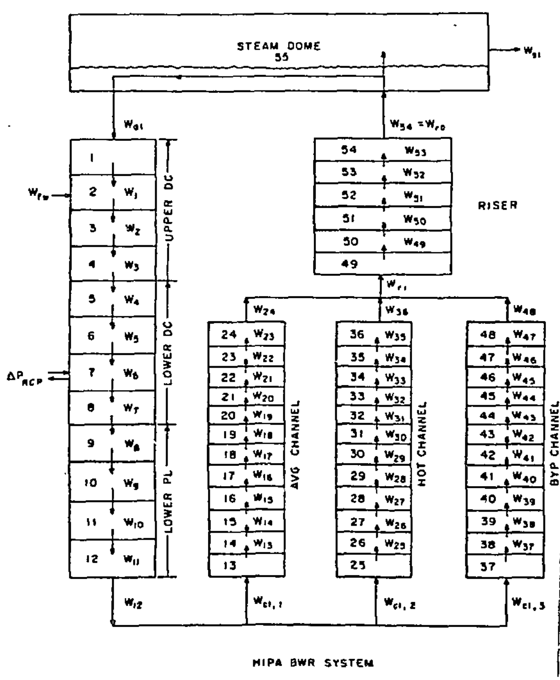

Figure 2 Vessel Flow Schematic and Arrangement of Computational Cells in Pressure Vessel

Thirty-seven different transients have been simulated as part of the developmental assessment for the plant analyzer, including sixteen multiple failure events. Geometric parameters, operating conditions and control parameters (delay times, amplifier gains etc.) were entered through keyboard commands. Failures were entered from a control panel shown in Figure 3.

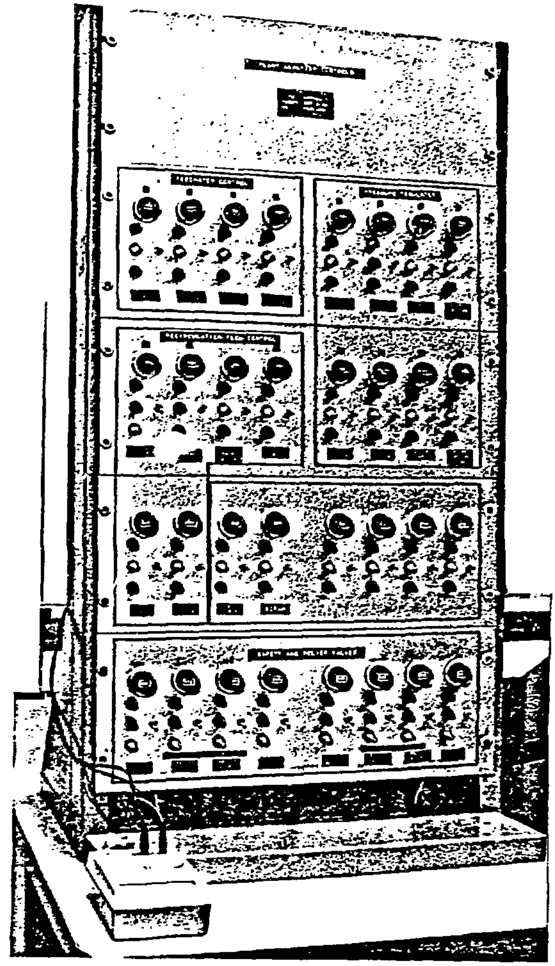

Figure 3 Control Panel

Simulation Speed

All transients can be simulated at speeds up to ten times faster than real process speed. It is easy to simulate as many as ten different transients in less than two hours and display the results on the IBM PC.

This simulation capability results from the plant analyzer's outstanding convenience for changing input data, from its ability to respond instantly to input changes, from its high simulation speed and from its graphic display capability which still can be further improved.

Simulation Accuracy

Good simulation accuracy can be achieved only with complete and exact plant-specific input data for geometric parameters, set point data for the plant protection system, control parameters and characteristics for pumps, valves, etc. A preliminary assessment of the plant analyzer has been performed with most input data as available for the Peach Bottom II BWR power plant. Unspecified data have been inferred from normal steady-state operating conditions and from data published in the Final Safety Analysis Report for Peach Bottom II.

Plant analyzer results have been compared [8] with results from CDC-7600 calculations using the same original equations, from the Final Safety Analysis Report, from GE calculations for ten different Anticipated Transients Without Scram in a generic BWR-4 plant, with results from TRAC-BD1, RELAP-5 and RAMONA-3B. The comparisons show relatively good agreement even though the transients were simulated with slightly different input data. Figures 4 through 10 show typical results of the comparisons between plant analyzer results and results from major systems codes. Figure 4 shows two pressure curves from TRAC-BD1 because the authors [11] observed an error in TRAC-BD1's kinetics calculations. Other differences are explained in more detail in reference [8].

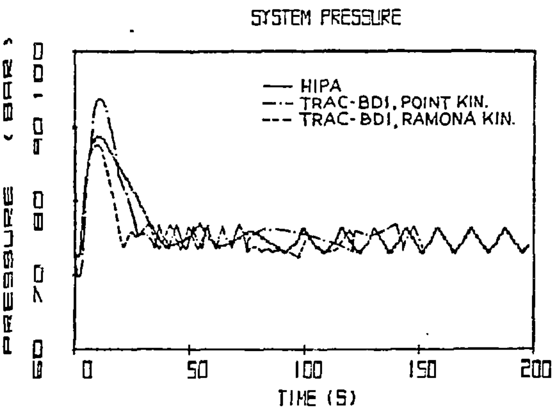

Figure 4 Comparison of System Pressure Predictions by Plant Analyzer and TRAC-BD1 Code

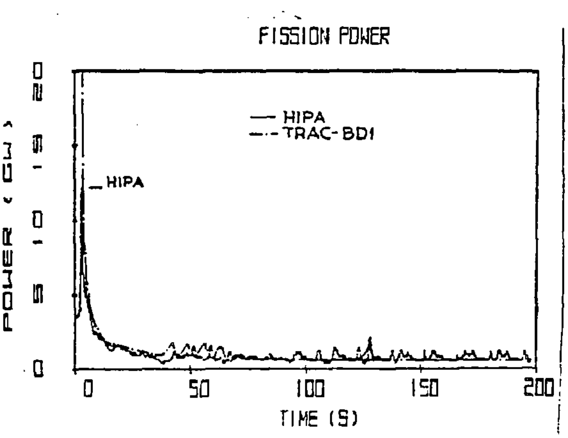

Figure 5 Comparison of System Pressure Predictions by Plant Analyzer and TRAC-BD1 Code

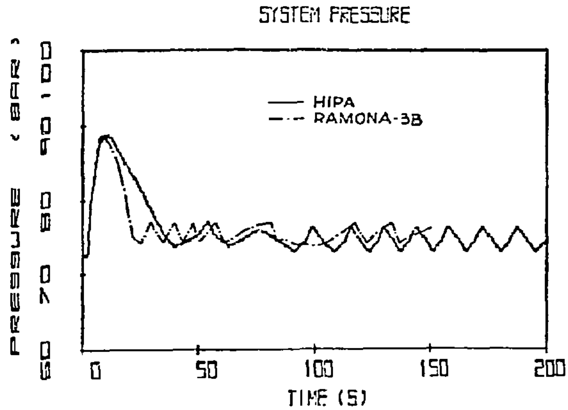

Figure 6 Comparison of Vessel Pressure Predictions from Plant Analyzer and RAMONA-3B Code

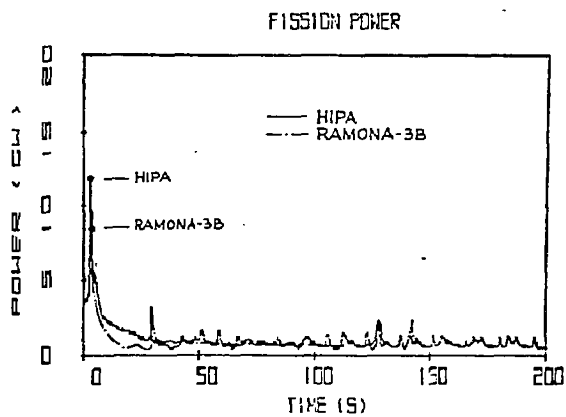

Figure 7 Comparison of Fission Power Predictions from Plant Analyzer and RAMONA-3B Code

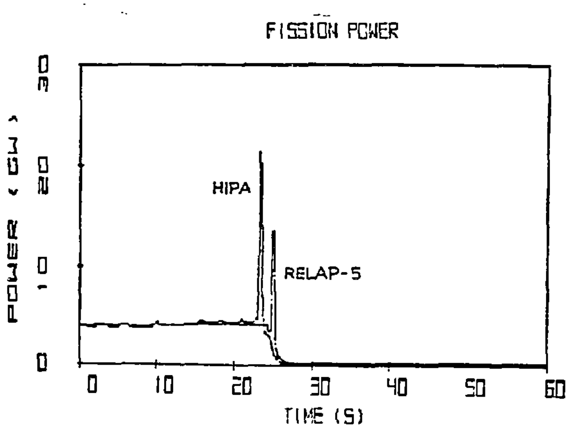

Figure 8 Comparison of Plant Analyzer with RELAP-5 Calculations for Failure of Feedwater Controller at Maximum Demand, Fission Power

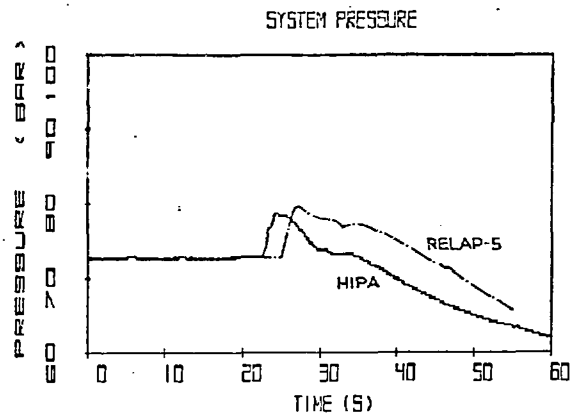

Figure 9. Comparison of Plant Analyzer Results with RELAP-5 Calculations for Failure of Feedwater Controller at Maximum Demand, System Pressure

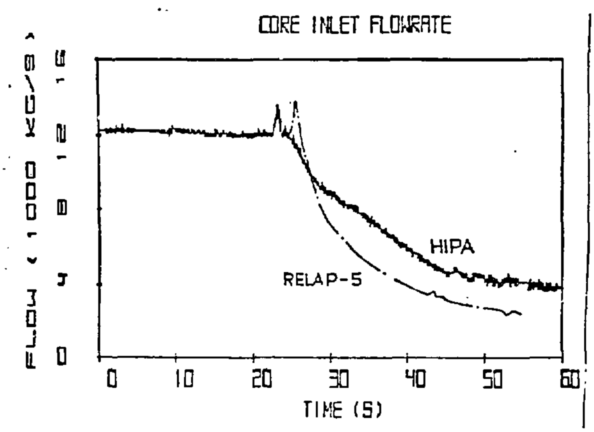

Figure 10 Comparison of Plant Analyzer Results with RELAP-5 Calculations for Failure of Feedwater Controller at Maximum Demand, Core Inlet Mixture Mass Flow Rate

CONCLUSIONS

BNL Plant Analyzer

It has been demonstrated that a combination of advanced modeling techniques and modern special-purpose array processor technology can yield a nuclear power plant simulation capability which is superior to that obtained on large mainframe computers, with standard FORTRAN systems codes.

Realistic and accurate simulations can be achieved with the plant analyzer at much faster than real-time simulation speeds, at low cost and with unsurpassed user convenience, for both normal and severe abnormal events.

The plant analyzer can accommodate hardware (controls and instruments) on-line into its computational loop and make the outside world part of its central core memory.

Computer-Aided Emergency Response

The new technology presented here produces the necessary simulation speed for plant monitoring, for failure diagnosis and for on-line predictions of the plant response to operator actions which might be contemplated for the mitigation of the consequences from reactor accidents.

A dedicated facility at the plant site, programmed for, and synchronized with, the specific power plant is required, in principle, for timely and effective emergency response. New research is required to accomplish the synchronization.

NOMENCLATURE

A	cross-sectional area
A_{min}	$Min\{A^+, A^-\}$
c	specific heat
C	heated perimeter
C_0	Zuber-Findley distribution parameter
C_g	geometric parameter
d_h	hydraulic diameter
$D_k/D\tau$	substantial derivative for phase k, k=g,ℓ
f_{FWH}	Eq. 19
f_1, f_2	Eq. 9
$f_{\ell o}$	single-phase friction factor
F_{pr}	property parameter
g_z	component of gravity in z-direction
G	mass flow rate
$\underline{h}$	enthalpy
h_c	convective heat transfer coefficient
j	volumetric flux
k	thermal conductivity
L	length
m	Eq. 20
m_g	vapor mass
$\mathcal{M}_j$	Eq. 7
n	Eq. 20
$N_{s,i}$	number of segments in j-th flow contour
p	pressure
q'_w	linear heating rate
q''_w	wall heat flux
q'''_ℓ	gamma heat absorption rate
r	radius
R_1	fuel pellet radius
R_m	mean cladding radius
R_w	outer cladding radius
s	cladding thickness
s_m	mixture entropy
T	temperature
u	internal energy
U	overall heat transfer coefficient
U_1	rotor entrance speed
v	specific volume
$\langle\langle V_{gj}\rangle\rangle$	void fraction-weighted, area-averaged drift velocity
V_v	vessel volume, V_1+V_2
V_1	volume of pure liquid in vessel
V_2	$V_v - V_1$
w	axial velocity component
W	mass flow rate
z	axial coordinate
α	void fraction
Γ_v	vapor generation rate per unit of volume
ζ	form loss coefficient
μ	W_{fw}/W_{SHS}
ν	$U_1/\sqrt{2\Delta h_{is}}$
ρ	density
τ	time
$\phi^2_{\ell o}$	two-phase multiplier for wall shear

Subscripts

c	condenser
cℓ	cladding
D	drain cooler
e	exit
f	saturated liquid
fℓ	fuel
fw	feedwater
g	saturated vapor
i	inlet
ij	loop and segment indices
inj	injection
is	isentropic
j	loop index
JTP	jet pump
ℓ	saturated liquid
m	two-phase mixture
s	saturated
sℓ	steam line
SHS	shell side of heat exchanger
v	vapor
∞	coolant (subcooled, saturated or superheated)

Special Symbols

<>	average
·	time derivative
'	derivative with respect to pressure, along saturation line
+ -	up and downstream of expansion or contraction

REFERENCES

1. W. Wulff, "BWR Training Simulator, An Evaluation of the Thermohydraulic Models for its Main Steam Supply System," Informal Report, BNL-NUREG-29815, Department of Nuclear Energy, Brookhaven National Laboratory, Upton, N.Y. 11973, July 1981. 46pp.

2. Safety Code Development Group, "TRAC-PF1: An Advanced Best Estimate Computer Program for Pressurized Water Reactor Analysis," NUREG-CR-3567, LA-9944-MS, Los Alamos National Laboratory, Los Alamos, New Mexico 87545, February 1984, 578pp.

3. V.H. Ransom, et al., "RELAP5/MOD1 Code Manual, Volume 1: System Models and Numerical Methods," NUREG/CR-1826, EGG-2070, March 1982, 113pp.

4. S.L. Thompson, "Thermal/Hydraulic Analysis, Research Quarterly Report, October-December 1983," NUREG/CR-3329, 4 of 4, SAND-1171, R4; March 1984, 59pp; (see pp. 24-36).

5. R.T. Lahey, Jr., "Analytical Modules for Nuclear Reactor Simulators," Simulation Methods for Nuclear Power Systems, U.S. Nuclear Regulatory Commission and Electric Power Research Institute, Proceedings EPRI WS-81-212, May 1981, pp. 3-57 to 3-83.

6. B.L. Buzbee, "Vectorization of Algorithms for Solving Systems of Difference Equations," Simulation Methods for Nuclear Power Systems, U.S. Nuclear Regulatory Commission and Electric Power Research Institute, Proceedings EPRI WS-81-212, May 1981, pp. 4-79 to 4-87.

7. W. Wulff, "Major System Codes, Capabilities and Limitations," Simulation Methods for Nuclear Power Systems, U.S. Nuclear Regulatory Commission and Electric Power Research Institute, Proceedings EPRI WS-81-212, May 1981, pp. 5-1 to 5-19.

8. W. Wulff, H.S. Cheng, S.V. Lekach and A.N. Mallen, "The BNL Plant Analyzer," Final Report, Department of Nuclear Energy, Brookhaven National Laboratory, Upton, N.Y. 11973, NUREG/CR 3943, BNL-NUREG 51812, August 1984.

9. W. Wulff, "Lumped Parameter Models for Transient Conduction in Nuclear Reactor Components," Department of Nuclear Energy, Brookhaven National Laboratory, Upton, N.Y. 11973, NUREG/CR-1540, BNL-NUREG-51231, June 1980, 35pp.

10. E.J. Fadden, "The AD10 Digital Computer Designed for Time Critical Simulation," Simulation Methods for Nuclear Power Systems, U.S. Nuclear Regulatory Commission and Electric Power Research Institute, Proceedings EPRI WS-81-212, May 1981, pp. 4-17 to 4-29.

11. C.J. Hsu, L. Neymotin and P. Saha, "Analysis of Typical BWR/4 MSIV Closure ATWS Using RAMONA-3B and TRAC-BD1 Codes," Joint ASME/ANS Conference on Design, Construction and Operation of Nuclear Power Plants, Portland, Oregon; ASME Paper No. 84-NE-10, (1984).